



## Preparation, Characterization, Theoretical and Biological Study of new Complexes with mannich base , 2chloro -N-5-(Piperidin -1-ylmethylthio)-1, 3, 4- Thiadiazol-2-yl)acetamide

**Noor Ali Hasan**

Department of Chemistry , College of Science for Women, University of Baghdad, Baghdad, Iraq.  
[nour.ali1205a@cs.w.uobaghdad.edu.iq](mailto:nour.ali1205a@cs.w.uobaghdad.edu.iq)

**Shaymaa R. Baqer**

Department of Chemistry , College of Science for Women, University of Baghdad, Baghdad, Iraq.  
[shyma0213@gmail.com](mailto:shyma0213@gmail.com)

**Article history: Received 23 August 2022, Accepted 25 September 2022, Published in January 2023.**

[doi.org/10.30526/36.1.2983](https://doi.org/10.30526/36.1.2983)

### Abstract

A new Mannich base ligand was prepared by reacting the 2-chloro.-N-(5-mercapto-1, 3, 4-thiadiazol -2-yl) acetamide and Piperidine in the presence (formaldehyde) (L) ligand. A series of ligand complexes were prepared from (L) with the metal ion Co (II), Ni (II), Cu (II), Pd (II), Pt (IV), and Au (III). Various spectroscopic techniques such as C.H.N.S, FTIR, UV-VIS, <sup>1</sup>HNMR, <sup>13</sup>CNMR, Magnetic moment, and molar conductivity successfully characterize the obtained compounds. The M: L ratio was determined using the molar ratio method in solution. All prepared compounds' antibacterial and antifungal activity was studied against two types of bacteria and one type of fungi at a rate of 0.02M. The standard  $\Delta H^{\circ}_f$  and  $\Delta E_b$  of the ligands and all the prepared complexes were calculated using Hyperchem 8.0.7 program, and the study proved that the complexes are more stable than the ligands. In addition, the vibrational frequencies of the ligand were calculated, and the theoretical error rate of the process was calculated.

**Keywords:** Transition Metal Complexes, Mannich Base, 1,3,4-thiadazole Antibacterial and Antifungal.

## 1. Introduction

The thiosemicarbazide compound with the molecular formula ( $\text{CH}_5\text{N}_3\text{S}$ ) and its complexes are of great biological importance due to their wide uses [1]. The compound thiodiazole compound with the molecular formula ( $\text{C}_2\text{H}_2\text{SN}_2$ ) is a heterogeneous compound because it contains two atoms of Carbon, Two atoms of nitrogen, and one sulfur atom [2]. Two nitrogen atoms and the sulfur atom are electron-donating [3] and are essential ligands in complexes when they bond with metal elements [2]. It has several types, one of which is the compound 1,3,4-thiadiazole, which is applied as anti-tumor medicine. Several derivatives are used as carbonic anhydrase inhibitors and antiparkinsonian agents [3]. Industrial and biological in the medical field, compound 1,3,4 has many applications against bacteria [4], fungi [5], and cancer [6]. The Mannich reaction is of significant importance reactions in chemistry. It is a reaction that includes three or more components of a substance or solvent [7], and it is one of the early examples of a three-component reaction [8]. In the past years, the focus has been on the complexes of Mannich bases that have heterogeneous rings, taking into account the amino-methyl group and studying the relationship of structure, its effect on the biological activity as anticancer agents and toxic to cancer cells [9,10]. There was also a focus on studying their importance as antibacterial and antifungals [11], anticonvulsants, anti-inflammatory [9], analgesic, and antioxidant activities [10]. The complexes of Mannich 's bases are essential and have wide applications in the medical and biological fields [11]. They are used as antioxidants [10], anticancer, antibacterial, and antifungal [12], and they have proven their effectiveness in all biological and medical fields [13].

## 2. Materials and Methods

In this paper, high-purity chemicals were used. CHNS elemental data were measured using an Eager300 elemental analyzer. The mineral content was determined using a Shimadzu 670 Flam Atomic Absorber Spectrophotometer. Conductivity data were acquired at  $10^{-3}$  M in the DMF solution of the complexes using a WTW conductance meter at 25 °C. FT-IR spectra were measured with a Shimadzu and Perkin Elmer FT infrared spectrophotometer using CsI (4000-200)  $\text{cm}^{-1}$ . Tablet. Absorption in the UV-visible region was recorded in ethanol solution using UV-Vis. Shimadzu Spectrophotometer 1800pcs. The magnetic susceptibility measurement of the complexes was carried out using the Faraday method, and the magnetic correction factor (D) was calculated using the Pascal constants of the atoms that made up the prepared complexes and the Brukar Magent BM6 device.  $^1\text{H}$ ,  $^{13}\text{C}$ NMR for compounds were at 25 °C using the Brukar400MHz . The grade of all prepared compounds was measured by Gallen Kamp MF.B-6.

### Preparation of starting material 2-amino 5-mercapto 1,3,4 thiadiazole (S1)

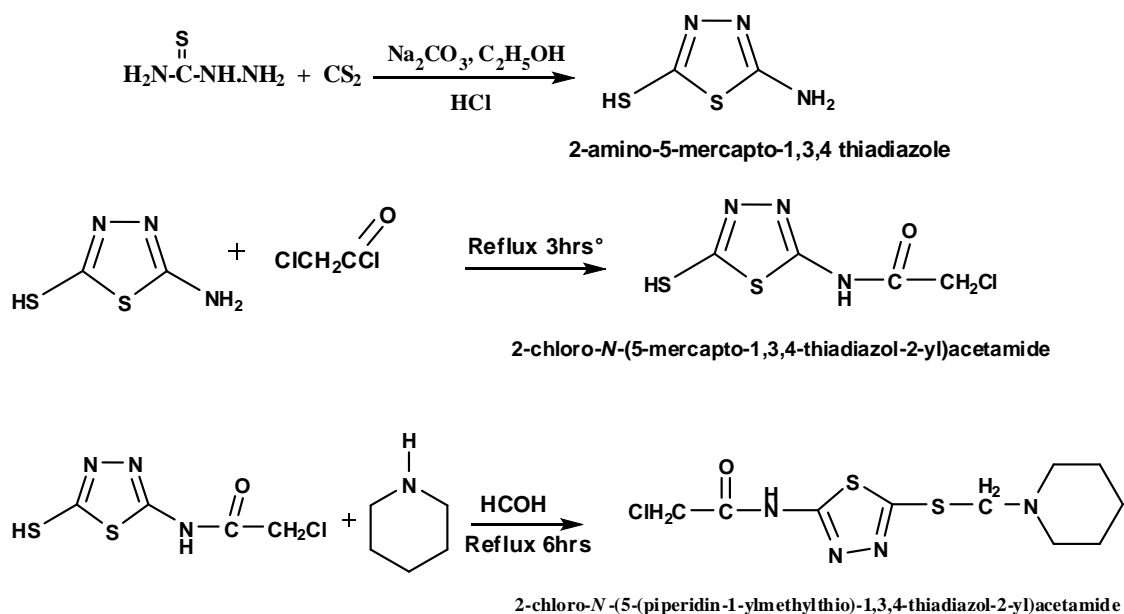
In a round bottom flask, (2gm,0.02mol) of thiosemicarbazide was dissolved in (25ml) ethanol (0.016gm,0.0002mol) of anhydrous sodium carbonate. (4.712 gm, 0.062 mol) of ( $\text{CS}_2$ ) was added with stirring and heating at ( $40\text{C}^0$ ) for an hour. Then, the mixture was raised for 7 hours after the solvent was evaporated (50ml) in distilled water, and drops of concentrated hydrochloric acid were added. A greenish-yellow was the precipitate. The color of the precipitate (was yellowish white, with a melting point of (229-231)  $\text{C}^0$  and the molecular formula ( $\text{C}_2\text{H}_3\text{N}_3\text{S}_2$ ) [14]. The sediment was washed, and the precipitate was filtered with a quantity of distilled water to get rid of the excess acid. It was recrystallized with the solvent ethanol.

### Preparation of 2-chloro-N-(5-mercapto-1,3,4-thiadiazol-2-yl)acetamide (S2)

Dissolved (0.1 gm, 0.01M) of 2-amino 5-mercapto 1,3,4 thiadiazole (S1) in ethanol was added with stirring (0.1 g, 0.02M) of chloroacetyl chloride) in an ice bath. The mixture was refluxed with heating for 3 hours. The resulting precipitate was washed with distilled water and recrystallized with ethanol. A yellowish-white precipitate was obtained with a molecular formula  $C_4H_4N_3S_2OCl$  and a melting point of (250-253)  $C^0$ .

### Synthesis of 2- Chloro –N-5-(Piperidine1-ylmethylthio)-1,3,4- Thiadiazol-2-yl)acetamide Ligand (Mannich ligand)(L )

Dissolved of (0.145 gm, 0.04M) of 2-chloro-N-(5-mercapto-1,3,4-thiadiazol-2-yl)acetamide in (10ml) of ethanol solvent was added with stirring and cooling (8ml) from formaldehyde and (0.08g, 0.03M) Piperidine. The mixture was refluxed and heated for six hours, leaving the solution to dry. The sediment was recrystallized in ethanol. The precipitate has a brown color, a molecular formula  $C_{10}H_{15}ClN_4OS_2$ , and a melting point of over 300  $C^0$ .



**Scheme 1.** Synthesis of Mannich Base, 2chloro –N-5-(Piperidin -1-ylmethylthio)-1, 3, 4- Thiadiazol-2-yl)acetamide (L)

## 2.2. Synthesis of Complexes

In the presence of ethyl alcohol solvent, some Mannich base complexes can be prepared. The ratio 1:1 of  $CoCl_2 \cdot 6H_2O$ ,  $NiCl_2 \cdot 6H_2O$ ,  $CuCl_2 \cdot 2H_2O$ ,  $PdCl_2$ ,  $H_2PtCl_6 \cdot 6H_2O$ , and  $HAuCl_4 \cdot H_2O$  and ligand. Then the mixture was refluxed for 3 hours. The resulting solids compounds were filtered off, washed with distilled water and ethanol, and dried in a desiccator. Some physical properties can be observed in **Table 1**.

**Table 1.** The physical properties of color and melting point in addition to the values of C.H.N.S and the percentage of all prepared compounds

| Comp.              | Color       | m.p / C <sup>0</sup> | Yield % | Atomic Abs.% Cal.(Found) | Elemental analysis Calc. (found) |                |                  |                  |
|--------------------|-------------|----------------------|---------|--------------------------|----------------------------------|----------------|------------------|------------------|
|                    |             |                      |         |                          | C                                | H              | N                | S                |
| <b>Mannich (L)</b> | Brown       | Over 300             | 76      | ----                     | 39.10<br>(38.66)                 | 4.88<br>(3.98) | 18.25<br>(19.01) | 20.85<br>(21.34) |
| <b>CoL</b>         | Dark green  | 118-120              | 80      | 12.22                    | 24.90<br>(23.78)                 | 4.15<br>(3.76) | 11.62<br>(12.78) | 13.28<br>(14.00) |
| <b>NiL</b>         | Light green | 182-185              | 76      | 11.96                    | 24.46<br>(25.11)                 | 3.87<br>(4.08) | 11.00<br>(10.94) | 13.04<br>(12.87) |
| <b>CuL</b>         | Dark brown  | 167-170              | 84      | 12.81                    | 24.22<br>(23.20)                 | 4.23<br>(5.12) | 10.90<br>(11.05) | 12.92<br>(13.67) |
| <b>PdL</b>         | Brown       | 218-221              | 67      | 32.06                    | 19.72<br>(18.77)                 | 2.46<br>(3.45) | 8.87<br>(9.11)   | 10.51<br>(11.41) |
| <b>PtL</b>         | Dark brown  | 202-205              | 74      | 21.88                    | 23.89<br>(24.02)                 | 3.38<br>(4.18) | 10.75<br>(11.44) | 12.74<br>(11.93) |
| <b>AuL</b>         | Green       | 212-215              | 77      | 32.27                    | 19.62<br>(18.56)                 | 2.45<br>(3.04) | 8.84<br>(9.94)   | 10.48<br>(11.05) |

### Theoretical study

In the theoretical study and using the hyperchem 8.0.7 program, the standard heat of formation and binding energy was calculated for all prepared compounds by PM3, ZINDO\I, and AMBER. The HOMO and LUMO were calculated to determine the active sites in the ligand molecule. The vibration frequencies were calculated theoretically for the ligand PM3 method, the practical results were compared with the theoretical results, and the error ratio between them was calculated, which was acceptable.

### Antibacterial and Antifungal activity

- 1.40 g of culture medium for bacteria and fungi was dissolved in a liter of distilled water, as the culture medium used for bacteria (Agar Mueller Hinton) and for fungi (Sabroid Dextroes Agar).
- 2.After dissolving by heating, the culture medium was placed in the sterilizer for 15 minutes, then poured into sterilized plastic dishes and left to solidify.
- 3.A hole was made using a cork drill with a diameter of 8 mm to add the material that inhibited the growth of bacteria and fungi.
- 4.The prepared ligands and complexes dissolved in DMSO at a concentration of 0.02M were injected into the pits of the culture medium.
- 5.The dishes were placed in the incubator at 37 °C for 24 hour for antibacterial activity and 72 hours for antifungal activity, then the inhibition diameters were measured using a ruler in mm for each of the prepared compounds.

### 3. Results and Discussion

All complexes were soluble in organic solvents DMF & DMSO. The ratio of metal-ligand was (1:1) the ligand, and their metal complexes were characterized: (FT-IR), (UV-vis) (<sup>1</sup>HNMR <sup>1</sup>HNMR and <sup>13</sup>CNMR, magnetic susceptibility, and conductivity.

**Fourier transforms spectroscopy (FT-IR) of Mannich ligand (L), and metal complexes**

FT-IR spectra of all prepared compounds were carried out in 4000 to 200  $\text{cm}^{-1}$ . The infrared spectra of Mannich ligand L and metal complexes appeared the active site number at 1701, 720, 1161, 2943, 2854, and 1620  $\text{cm}^{-1}$  which was due to  $[(\nu_{\text{C=O}})_{\text{b}}, (\nu_{\text{C-S}})]_{\text{b}}, (\nu_{\text{C-S}})_{\text{b}}, (\nu_{\text{C-H}_2\text{N}})$  and  $\text{C}=\text{N}_{1,3,4\text{thio}}$  sequentially [15]. When a metal ion was bonded to the ligand through the nitrogen atom of  $\text{C}=\text{N}_{1,3,4\text{thio}}$  absorption bands shifted towards frequencies within the range (1602-1658)  $\text{cm}^{-1}$  in cobalt, nickel, copper, palladium, platinum, and gold complexes, respectively. In other absorption bands, the carbonyl group ( $\text{C}=\text{O}$ ) has been shifted according to the frequencies (1728, 1728, 1691, 1690, 1686, 1722)  $\text{cm}^{-1}$ . In all the prepared complexes oxygen of carbonyl,  $\nu_{\text{C}=\text{O}}$  took place in coordination. This supported compatibility with the  $\text{C}=\text{O}$  group [16]. We also noticed a shift in C-S and CSC groups for each of the Co(II), Ni(II), Cu(II), Pd(II), Pt(IV), and Au(III) complexes, which indicated the occurrence of coordination through them. According to these results, the coordination made of this ligand was predicted as a tridentate through  $\nu_{\text{C}=\text{N}}$ ,  $\nu_{\text{C}=\text{O}}$  group, and sulfur [17]. Other bands could be attributed to  $\nu_{\text{M}-\text{N}}$ ,  $\nu_{\text{M}-\text{O}}$ ,  $\nu_{\text{M}-\text{S}}$ , and  $\nu_{\text{M}-\text{Cl}}$  for complexes [13]. Other bands can be shown in **Table 2**. Also, other bands belonging to the  $\nu_{\text{NH}}$  group and the  $\nu_{\text{CH}_2-\text{N}}$  group appeared that they did not have a displacement when the coordination occurred, indicating non-coordination through them [16].

**Table 2.** The main absorption bands of the infrared spectrum of ligand (L), and its metal complexes ( $\text{cm}^{-1}$ )

| COMP.      | $\nu_{\text{C}=\text{O}}$ | $\nu_{\text{CH}_2-\text{N}}$ | $\nu_{\text{C}=\text{N}}$<br>1,3,4thio. | $\nu_{\text{CSC}}$ | $\nu_{\text{CS}}$ | $\nu_{\text{M}-\text{O}}$ | $\nu_{\text{M}-\text{N}}$ | $\nu_{\text{M}-\text{S}}$ | $\nu_{\text{M}-\text{Cl}}$ |
|------------|---------------------------|------------------------------|---|--------------------|-------------------|---------------------------|---------------------------|---------------------------|----------------------------|
| <b>L</b>   | 1701                      | 2943<br>2854                 | 1620                                    | 1161               | 702               | ----                      | ----                      | ----                      | ----                       |
| <b>CoL</b> | 1728                      | 2943<br>Broad                | 1602                                    | 1145               | 678               | 586                       | 520                       | 478                       | 345                        |
| <b>NiL</b> | 1728                      | 2943                         | 1658                                    | 1153               | 686               | 547                       | 513                       | 416                       | 337                        |
| <b>CuL</b> | 1691                      | 2942                         | 1639                                    | 1175               | 729               | 590                       | 513                       | 470                       | 320                        |
| <b>PdL</b> | 1690                      | 2947<br>2854                 | 1608                                    | 1171               | 77                | 540                       | 520                       | 482                       | 345                        |
| <b>PtL</b> | 1686                      | 2943<br>2858                 | 1608                                    | 1190               | 744               | 559                       | 516                       | 451                       | 310                        |
| <b>AuL</b> | 1722                      | 2947                         | 1639                                    | 1188               | 786               | 540                       | 516                       | 470                       | 337                        |

**Uv-vis Spectra, Magnetic susceptibility and molar conductivity**

The electronic spectra of all prepared compounds are shown in **Table (3)**. The UV-vis spectrum of the free ligand displayed a sharp band at (25773)  $\text{cm}^{-1}$  is attributed to  $n \rightarrow \pi^*$  transition. Transitions appeared in the region (33112)  $\text{cm}^{-1}$  and 37314  $\text{cm}^{-1}$  is attributed to  $\pi \rightarrow \pi^*$  transitions [18].

In the UV- visible spectrum of dark green Co (II) complex, two peaks were observed at (10240, 19230  $\text{cm}^{-1}$ ) dedicated to  ${}^4\text{T}_{1g} \rightarrow {}^4\text{T}_{2g}$ ,  ${}^4\text{T}_{1g} \rightarrow {}^4\text{T}_{2g(p)}$  transitions sequentially and (28659, 41838)  $\text{cm}^{-1}$ . It was due to the transition  $\text{IL} \rightarrow \text{Co CT}$ , which indicated the octahedral geometry of Co (II). Magnetic moment. (4.00) B.M showed a higher orbital contribution. Conductivity measurement in DMF (67  $\mu\text{S}\cdot\text{cm}^{-1}$ ) showed that the complex was ionic. The electronic spectrum of this complex can be seen in **Table (3)** [19].

In the UV- visible of Ni (II) complex, three peaks were observed at (10582, 15772, 24875  $\text{cm}^{-1}$ ). They were dedicated to  ${}^3\text{A}_{2g} \rightarrow {}^3\text{T}_{2g}$ ,  ${}^3\text{A}_{2g} \rightarrow {}^3\text{T}_{1g(f)}$ ,  ${}^3\text{A}_{2g} \rightarrow {}^3\text{T}_{1g(p)}$  sequentially and (26109, 40983)  $\text{cm}^{-1}$  was due to  $\text{IL} \rightarrow \text{NiCT}$  which indicated the octahedral geometry of Ni. The magnetic moment, (3.09) B.M showed a higher orbital contribution [20] Conductivity measurement in DMF (21  $\mu\text{S}\cdot\text{cm}^{-1}$ ) appearing that the complex was nonionic [19]. Light Green complex showed paramagnetic and high spin octahedral. The electronic spectrum of this complex can be seen in **Table (3)**.

In the UV- visible region of the Cu(II) complex, one peak was observed at (15197  $\text{cm}^{-1}$ ), dedicated to  ${}^2\text{E}_g \rightarrow {}^2\text{T}_{2g}$ , and (27629, 29069, 42918)  $\text{cm}^{-1}$  was due to IL  $\rightarrow$  CuCT which indicated the octahedral geometry of Cu (II) [20]. Magnetic moment, (1.78) B.M [21]. Conductivity measurement in DMF (61  $\mu\text{S}\cdot\text{cm}^{-1}$ ) showed that the complex was ionic. Dark brown complex showed paramagnetic and high spin octahedral. The electronic spectrum of this, complex can be seen in **Table (3)**.

In the UV-visible region of the Pd (II) complex, one peak was observed at (24038 $\text{cm}^{-1}$ ), dedicated to  ${}^1\text{A}_{1g} \rightarrow {}^1\text{B}_{1g}$  transition, and (31446, 45248)  $\text{cm}^{-1}$  was due to IL  $\rightarrow$  PdCT, which indicated square planer geometry of Pd (II) [19]. Magnetic moment (0) B.M. Conductivity measurement in DMF (70  $\mu\text{S}\cdot\text{cm}^{-1}$ ) showed that the complex was ionic, low spin and square planer geometry [22]. The electronic spectrum of this complex can be seen in **Table (3)**.

In the UV- visible region of the Pt(II) complex two peaks were observed at (10812, 12050  $\text{cm}^{-1}$ ) was assigned to  ${}^1\text{A}_{1g} \rightarrow {}^3\text{T}_{2g}$ , (23980  $\text{cm}^{-1}$ ) was assigned to  ${}^1\text{A}_{1g} \rightarrow {}^1\text{T}_{1g}$ , transitions which indicated the octahedral geometry of Pt (IV). Magnetic moment, (0) B.M [23]. Conductivity measurement in DMF (69  $\mu\text{S}\cdot\text{cm}^{-1}$ ) showed that the complex was ionic [24].

In the UV- visible region of the Au (III) complex, two peaks were observed at (251889, 30030 $\text{cm}^{-1}$ ) dedicated to  ${}^1\text{A}_{1g} \rightarrow {}^1\text{B}_{1g}$  and  ${}^1\text{A}_{1g} \rightarrow {}^1\text{E}_g$  transitions sequentially and (40983)  $\text{cm}^{-1}$  was due to IL  $\rightarrow$  AuCT which indicated the square planner geometry Au (III). The magnetic moment was (0) B.M [25]. The conductivity measurement in DMF was (88  $\mu\text{S}\cdot\text{cm}^{-1}$ ) [22]. This complex was ionic, low spin and square planer geometry. The electronic spectrum of this complex can be seen in **Table 3** [26].

**Table 3.** The electronic spectra,  $\mu_{\text{eff}}$  of complexes, conductivity and suggested geometry for ligand and its metal complexes

| Comp. | Absorption $\text{Cm}^{-1}$                         | Assignments   | $\mu_{\text{e}}^{\text{eff}}$ B.M. | Conductivity $\mu\text{S}\cdot\text{cm}^{-1}$ | Suggested geometry |
|-------|---|---|------------------------------------|---|--------------------|
| L     | 25773<br>33112<br>37314                             | $n \rightarrow \pi^*$<br>$\pi \rightarrow \pi^*$<br>$\pi \rightarrow \pi^*$   | ----                               | ----  | ----               |
| CoL   | 10240<br>19230<br>28659<br>41838                    | ${}^4\text{T}_{1g} \rightarrow {}^4\text{T}_{2g}$<br>${}^4\text{T}_{1g} \rightarrow {}^4\text{T}_{1g(\text{p})}$<br>IL $\rightarrow$ CoCT<br>IL $\rightarrow$ CoCT  | 4.00<br>(3.87)                     | 67  | Octahedral         |
| NiL   | 10582<br>15772<br>24875<br>26109<br>40983           | ${}^3\text{A}_{2g} \rightarrow {}^3\text{T}_{2g}$<br>${}^3\text{A}_{2g} \rightarrow {}^1\text{T}_{1g(\text{F})}$<br>${}^3\text{A}_{2g} \rightarrow {}^3\text{T}_{1g(\text{p})}$<br>IL $\rightarrow$ Ni CT<br>IL $\rightarrow$ Ni CT       | 3.09<br>(2.82)                     | 21  | Octahedral         |
| CuL   | 15197<br>27629<br>29069<br>42918                    | ${}^2\text{E}_g \rightarrow {}^2\text{T}_{2g}$<br>IL $\rightarrow$ Cu CT<br>IL $\rightarrow$ Cu CT<br>IL $\rightarrow$ Cu CT  | 1.78<br>(1.73)                     | 61  | Octahedral         |
| PdL   | 24038<br>31446<br>45248                             | ${}^1\text{A}_{1g} \rightarrow {}^1\text{B}_{1g}$<br>IL $\rightarrow$ Pd CT<br>IL $\rightarrow$ Pd CT   | 0.00                               | 73  | Square planer      |
| PtL   | 108551<br>12050<br>23980<br>26881<br>34602<br>45662 | ${}^1\text{A}_{1g} \rightarrow {}^3\text{T}_{2g}$<br>${}^1\text{A}_{1g} \rightarrow {}^3\text{T}_{1g}$<br>${}^1\text{A}_{1g} \rightarrow {}^1\text{T}_{1g}$<br>IL $\rightarrow$ Pt CT<br>IL $\rightarrow$ Pt CT<br>IL $\rightarrow$ Pt CT | 0.00                               | 69  | Octahedral         |
| AuL   | 25575<br>27624                                      | ${}^1\text{A}_{1g} \rightarrow {}^1\text{B}_{1g}$<br>${}^1\text{A}_{1g} \rightarrow {}^1\text{E}_g$<br>IL $\rightarrow$ Au CT   | 0.00                               | 88  | Square planer      |

### The $^1\text{H-NMR}$ spectra of 2-Chloro -N-5-(Piperidin-1-ylmethylthio)-1,3,4- thiadiazol-2-yl)acetimide

The  $^1\text{H-NMR}$  spectrum of the L can be observed in table 4 in DMSO- $d_6$ . The proton nuclear resonance ( $^1\text{H-NMR}$ ) spectrum of ligand showed some signals in ppm. Two signals appeared at (1.54, 1.64) ppm and another signals appeared at (2.42,2.43,2.45) ppm, attributed to the proton of Piperidin [11]. The Proton of  $\text{CH}_2\text{-N}$  and  $\text{CH}_2\text{-Cl}$  groups appeared at (4.49) ppm and (3.97) ppm. The signal at (12.39) ppm was attributed to proton of NH group **Table 4**.

### The $^{13}\text{C-NMR}$ Spectra of 2-Chloro -N-5-(Piperidine1-ylmethylthio)-1,3,4- thiadiazol-2-yl)acetimide

The  $^{13}\text{C-NMR}$  spectrum of ligand showed some signal. The signal at 43.7 can be assigned to carbon of ( $\text{CH}_2\text{-Cl}$ ) group. The signals at 23.1,24.4 and 54.1 ppm returned to carbon of  $\text{CH}_2$  of Piperidin and  $\text{CH}_2\text{-N}$  of Piperidin [3]. Other signals appeared at 163.2 and 168.4 can be assigned to carbon of ( $\text{C-S,1,3,4 thio.}$ ) group and carbon of carbonyl group, respectively [4]. Another peak can be observed in table 4.

**Table 4.**  $^1\text{H}$  and  $^{13}\text{C}$  nuclear magnetic resonance spectra of Mannich base ligand (L)

| $^1\text{H-NMR}$   | $^{13}\text{C-NMR}$   |
|--|---|
| $^1\text{H-NMR}$ (DMSO- $d_6$ ) $\delta$ ppm:2.42,2.43,2.45 (d,2H, $\text{CH}_2$ of Piperidine) 1.64 and 1.54 (d,2H, $\text{CH}_2$ of Piperidine) ,12.39 (S,H,NH) of amide, 3.97,4.49 (S,H, $\text{CH}_2$ aliphatic of $\text{CH}_2\text{-N}$ and $\text{CH}_2\text{-Cl}$ respectively | <b>Mannich (L) :</b><br>$^{13}\text{C-NMR}$ (DMSO- $d_6$ ) $\delta$ ppm:43.7 ( $\text{CH}_2\text{-Cl}$ ), 23.1,24.4 ( $\text{CH}_2$ of Piperidine), 53.1 ( $\text{CH}_2\text{-N}$ of Piperidine) ,54.1 ( $\text{CH}_2\text{-N}$ ) of methylene group, 163.2 (S-C of 1,3,4 thiadiazole group ,168.4 (C=O group). |

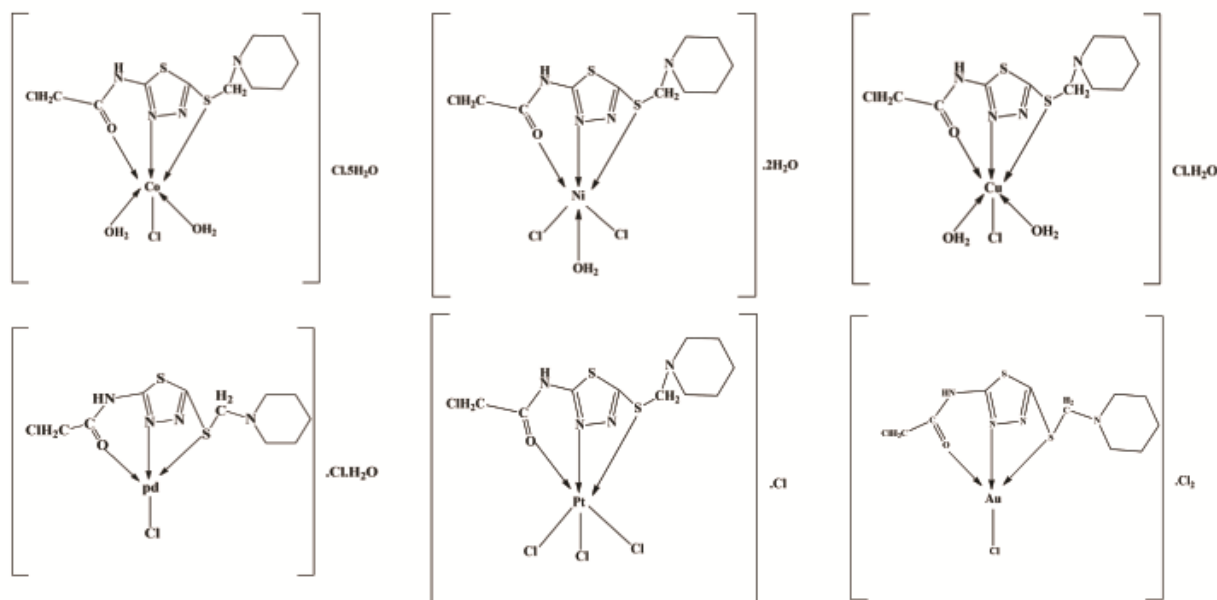


**Figure 1.** The proposed geometry of the prepared complexes

### Molar ratio Method

In the solution state, the ratio metal to ligand can be calculated using molar ratio method at the maximum wavelength, and at concentration  $1 \times 10^{-3}$  of all the prepared complexes. The results proved that the ratio of metal to ligands was (1:1).

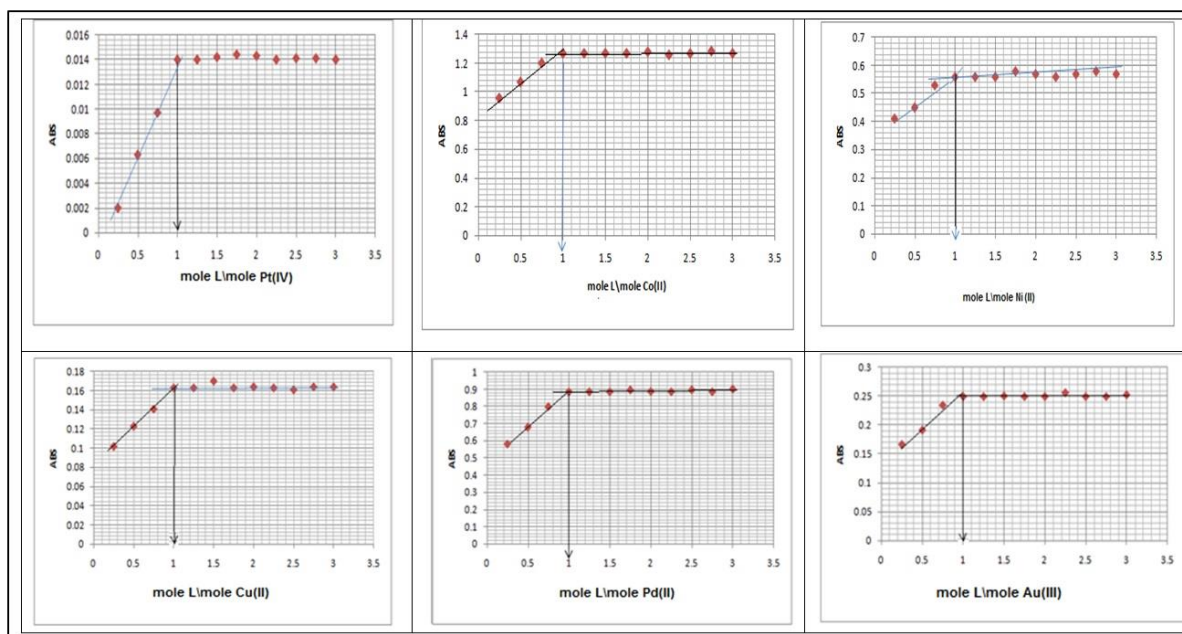


Figure 2. Molar ratio plot of, L metal complexes

### 4. Antibacterial and antifungal Activity

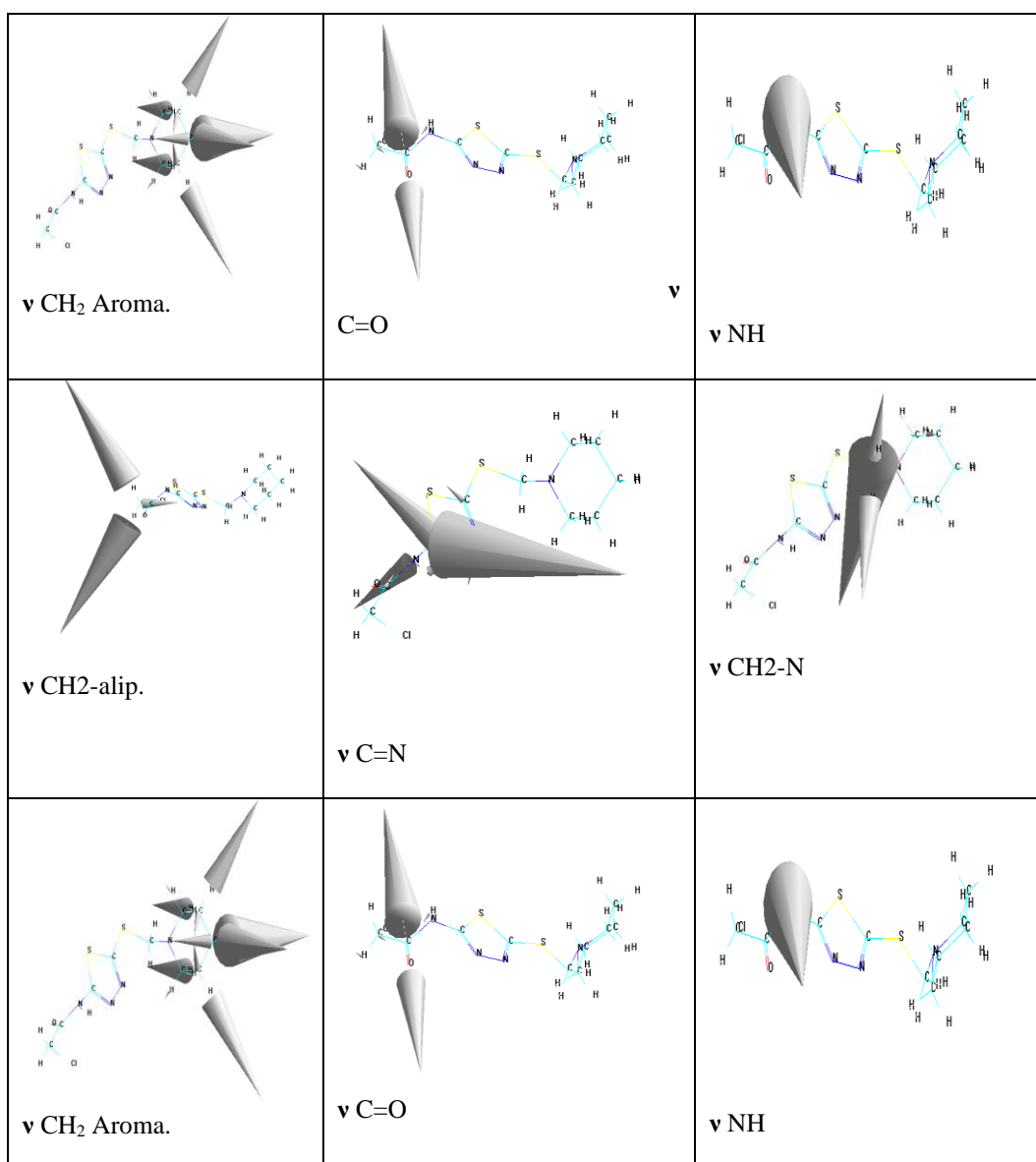
The biological activity of all prepared compounds was tested by two types of bacteria and one type of fungi at a concentration of 0.02M. The results obtained for the antibacterial and antifungal of the Mannich ligand and its new complexes are presented in **Table 5**. The diameter of the inhibition zone was measured in (mm) using amoxicillin and metronidazole as standard drugs for bacteria and fungi, respectively. The ligand and complexes generally showed moderate activity, and some were high towards bacteria and fungi tested. The nickel complex showed higher activity against all bacteria and fungi than standard drugs. This would suggest that the chelation could facilitate the ability of a complex to cross-brand into the cell wall of bacteria and fungi and kill them [27].

Table 5. Antibacterial activity of L and its Metal Complexes at 0.02 M

| Compounds |               | Inhibition Zone (mm.) |                 |               |                   |                |
|-----------|---------------|-----------------------|-----------------|---------------|-------------------|----------------|
|           |               | Gram Positive         |                 | Gram negative |                   | Fungi          |
|           |               | <i>staph</i>          | <i>Bacillus</i> | <i>E.coli</i> | <i>Klebsiella</i> | <i>Candida</i> |
| 1         | CoL           | 27                    | 29              | 16            | 20                | 24             |
| 2         | NiL           | 35                    | 27              | 32            | 22                | 27             |
| 3         | CuL           | 21                    | 18              | 22            | 14                | 18             |
| 4         | PdL           | 18                    | 17              | 14            | 14                | 21             |
| 5         | PtL           | 20                    | 15              | 15            | 13                | 15             |
| 6         | AuL           | 20                    | 12              | 20            | 15                | 15             |
| 7         | DMSO          | -ve                   | -ve             | -ve           | -ve               | -ve            |
| 8         | L             | 28                    | 25              | 25            | 21                | 25             |
| 10        | Amoxicillin   | 12                    | 12              | 13            | 11                | ----           |
| 11        | Metronidazole | ----                  | ----            | ----          | ----              | 13             |

**Table 6.** The vibrational frequencies of L using HyperChem-8.0.7 program

| Symb.               | v(C=N) ring | vC=O   | vCSC   | vCH <sub>2</sub> -N | vCS    |
|---------------------|-------------|--------|--------|---------------------|--------|
| Experimental        | 1620        | 1701   | 1161   | 2854<br>2943        | 702    |
| Theoretical         | *1623       | 1768*  | 1190*  | 2928<br>2998*       | *739   |
| Percentage of error | (0.18)      | (3.78) | (2.43) | (-1.49)<br>(1.83)   | (5.00) |



**Figure 3.** Vibration spectra of ligand Mannich base (L)

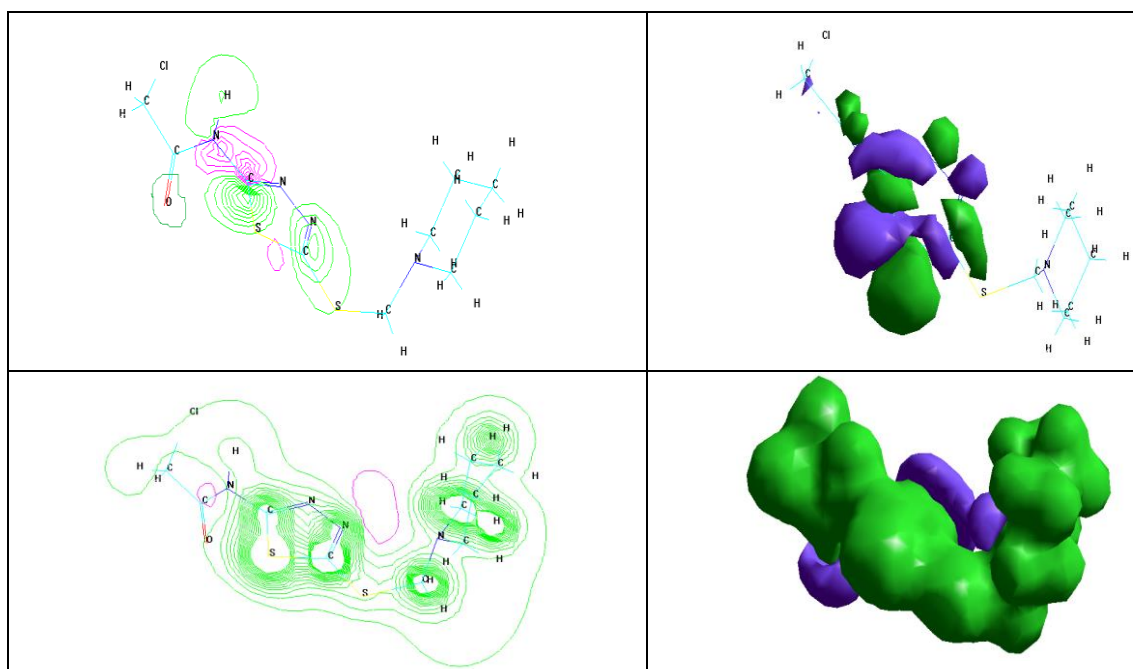


**Figure 4.** HOMO, LUMO and Electrostatic Potential of ligand L

**Table 7.** Heat of formation, binding energy (in  $\text{KJ.mol}^{-1}$ ) and dipole moment (in Debye) for ligand, (L) and its metal complexes using HyperChem-8.0.7 program

| Comp. | PM3                |              |       | ZINDO/1            |              |       | AMBER                           |       |
|-------|--------------------|--------------|-------|--------------------|--------------|-------|---------------------------------|-------|
|       | $\Delta H_f^\circ$ | $\Delta E_b$ | $\mu$ | $\Delta H_f^\circ$ | $\Delta E_b$ | $\mu$ | $\Delta E_b = \Delta H_f^\circ$ | $\mu$ |
| L     | 17.09737           | 3146.68162-  | 1.73  | -8705.7206         | -12205.5026  | 3.23  | ----                            | ----  |
| CoL   | 330.3585-          | 3953.05357-  | 4.78  | -6958.85848        | -10581.55348 | 9.57  | ----                            | ----  |
| NiL   | 185.61811-         | -3673.94011  | 4.32  | -6893.90242        | -10382.22442 | 6.30  | ----                            | ----  |
| CuL   | 175.42755-         | 3776.42255-  | 2.22  | -6999.43292        | -10600.42792 | 5.17  | ----                            | ----  |
| PdL   | ----               | ----         | ----  | ----               | ----         | ----  | 88.4691                         | 3.35  |
| PtL   | ----               | ----         | ----  | ----               | ----         | ----  | 255.7924                        | 4.06  |
| AuL   | ----               | ----         | ----  | ----               | ----         | ----  | 89.5963                         | 3.22  |

## 5. Conclusion

Mannich base ligand complexes have been successfully synthesized using the conventional method. The assembly of the six proposed complexes was successfully achieved by the procedures previously described. The results obtained from this investigation were obtained according to the data presented by the physical and chemical analysis. The results showed that the complexes have an octahedral geometry for the cobalt, nickel, copper, and platinum complexes and a square-planer geometry for the palladium and gold complexes. Ni complex showed good activity against positive and negative bacteria and fungi compared to amoxicillin and metronidazol. The standard heat of formation and binding energy was calculated using the hyperchem 8.0.7 program, proving that the complexes are more stable than the ligand.

## References

1. Jia, X.; Liu, Q.; Wang, S.; Zeng, B.; Du, G.; Zhang, C.; Li, Y. Synthesis, Cytotoxicity, and in Vivo Antitumor Activity Study of Parthenolide Semicarbazones and Thiosemicarbazones. *Bioorganic & Medicinal Chemistry* **2020**, *28*, 115557, doi:10.1016/j.bmc.2020.115557.
2. Roder, C.; Thomson, M.J. Auranofin: Repurposing an Old Drug for a Golden New Age. *Drugs R D* **2015**, *15*, 13–20, doi:10.1007/s40268-015-0083-y.
3. Jain, A.K.; Sharma, S.; Vaidya, A.; Ravichandran, V.; Agrawal, R.K. 1,3,4-Thiadiazole and Its Derivatives: A Review on Recent Progress in Biological Activities. *Chemical Biology & Drug Design* **2013**, *81*, 557–576, doi:10.1111/cbdd.12125.
4. Ainsworth, C. The Condensation of Aryl Carboxylic Acid Hydrazides with Orthoesters. *J Am Chem Soc* **1955**, *77*, 1148–1150, doi:10.1021/ja01610a019.
5. de Andrade Danin Barbosa, G.; Palermo de Aguiar, A. Synthesis of 1,3,4-Thiadiazole Derivatives and Microbiological Activities: A Review. *Revista Virtual de Química* **2019**, *11*, 806–848, doi:10.21577/1984-6835.20190058.
6. Pandey, A.; Rajavel, R.; Chandraker, S.; Dash, D. Synthesis of Schiff Bases of 2-Amino-5-Aryl-1,3,4-Thiadiazole and Its Analgesic, Anti-Inflammatory and Anti-Bacterial Activity. *E-Journal of Chemistry* **2012**, *9*, 2524–2531, doi:10.1155/2012/145028.
7. Schweinfurth, D.; Krzystek, J.; Schapiro, I.; Demeshko, S.; Klein, J.; Telser, J.; Ozarowski, A.; Su, C.-Y.; Meyer, F.; Atanasov, M.; et al. Electronic Structures of Octahedral Ni(II) Complexes with “Click” Derived Triazole Ligands: A Combined Structural, Magnetometric, Spectroscopic, and Theoretical Study. *Inorganic Chemistry* **2013**, *52*, 6880–6892, doi:10.1021/ic3026123.
8. G. Pyne, S.; Tang, M. The Boronic Acid Mannich Reaction. In *Organic Reactions*, John Wiley & Sons, Inc.: Hoboken, NJ, USA, **2013**, 211–498.
9. Singh, B.N.; Shukla, S.K.; Singh, M. Synthesis and Biological Activity of Sulphadiazine Schiff Bases of Isatin and Their N-Mannich Bases. *asian Journal of chemistry* **2007**, *19*, 5013.
10. Sumrta, S.H.; Arshad, Z.; Zafar, W.; Mahmood, K.; Ashfaq, M.; Hassan, A.U.; Mughal, E.U.; Irfan, A.; Imran, M. Metal Incorporated Aminothiazole-Derived Compounds: Synthesis, Density Function Theory Analysis, in Vitro Antibacterial and Antioxidant Evaluation. *Royal Society Open Science* **2021**, *8*, doi:10.1098/rsos.210910.
11. Rehman, M. ur Metal-Based Antimicrobial Agents: Synthesis, Characterization and Biological Studies of Mannich Base Derivatives of Benzimidazole and Their Metal Complexes. *Science Journal of Chemistry* **2013**, *1*, 56, doi:10.11648/j.sjc.20130105.12.
12. Pishawikar, S.A.; More, H.N. Synthesis, Docking and in-Vitro Screening of Mannich Bases of Thiosemicarbazide for Anti-Fungal Activity. *Arabian Journal of Chemistry* **2017**, *10*, S2714–S2722, doi:10.1016/j.arabjc.2013.10.016.
13. Evans, A.; Kavanagh, K.A. Evaluation of Metal-Based Antimicrobial Compounds for the Treatment of Bacterial Pathogens. *Journal of Medical Microbiology* **2021**, *70*, doi:10.1099/jmm.0.001363.
14. Hadeel Hamid Mahmood, S.R.B. PREPARATION, PHYSICOCHEMICAL AND BIOLOGICAL STUDY OF SCHIFF BASE DERIVED FROM 2- AMINO-5-MERCPTO-1,3,4 THIADIAZOLE WITH SOME METAL IONS. *Biochem. Cell. Arch* **2021**.
15. Karcz, D.; Matwijczuk, A.; Kamiński, D.; Creaven, B.; Ciszakowicz, E.; Lecka-Szlachta, K. Starzak, K. Structural Features of 1,3,4-Thiadiazole-Derived Ligands and Their Zn(II) and Cu(II) Complexes Which Demonstrate Synergistic Antibacterial Effects with Kanamycin. *International Journal of Molecular Sciences* **2020**, *21*, 5735, doi:10.3390/ijms21165735.
16. Guo, J.; Zhou, J.; Guorui Fu; He, Y.; Li, W.; Lü, X. Two Efficient Near-Infrared (NIR) Luminescent [Ir(C<sup>N</sup>)<sub>2</sub>(N<sup>O</sup>)]-Characteristic Complexes with 8-Hydroxyquinoline (8-Hq) as the Ancillary Ligand. *Inorganic Chemistry Communications* **2019**, *101*, 69–73, doi:10.1016/j.inoche.2019.01.019.
17. Lotfi, S.; Brgoch, J. Predicting Pressure-Stabilized Alkali Metal Iridides: A–Ir (A = Rb, Cs). *Computational Materials Science* **2019**, *158*, 124–129, doi: 10.1016/j.commatsci.2018.11.018.

18. Guo, J.; Zhou, J.; Guorui Fu; He, Y.; Li, W.; Lü, X. Two Efficient Near-Infrared (NIR) Luminescent [Ir(C<sup>N</sup>)<sub>2</sub>(N<sup>O</sup>)]-Characteristic Complexes with 8-Hydroxyquinoline (8-Hq) as the Ancillary Ligand. *Inorganic Chemistry Communications* **2019**, *101*, 69–73, doi:10.1016/j.inoche.2019.01.019.
19. Ibraheem, I.H.; Sadiq, A.S.; Al-Tameemi, M.; Alias, M.F. Synthesis, Spectral Identification, Antibacterial Evaluation and Theoretical Study of Co, Fe, Rh and Pd Complexes for 2-Benzoylthiobenzimidazol. *Baghdad Science Journal* **2022**, 1326–1334, doi:10.21123/bsj.2022.6704.
20. Baqer, S.R.; Hassan, S.S.; Hassan, N.M.; Saleh, A.M. Biological Evaluation and Theoretical Study of Bi-Dentate Ligand for Amoxicillin Derivative with Some Metal Ions. *Baghdad Science Journal* **2021**, *18*, doi:10.21123/bsj.2021.18.4.1269.
21. Gülfen, M.; Özdemir, A. Monitoring Cu(II)-Insulin and Mn(II)-Insulin Complexes Using Potentiometric, Chromatographic, UV–Vis Absorption and Fluorescence Emission Spectroscopic Techniques. *Journal of Molecular Structure* **2022**, *1259*, 132763, doi:10.1016/j.molstruc.2022.132763.
22. Alias, M.F.; Murtadha, J.H.; Abdul ALrazzaq, I.H. Study of Cytotoxic Effect of Aqueous Extract Fenugreek (Trigonella Foenum Graecum L.S) Seeds and The New Complexes of Rh (II) and Pd (II) on Cancer Cell Lines . *Baghdad Science Journal* **2018**, *9*, 289–295.
23. Mortazavi, S.Z.; Parvin, P.; Reyhani, A.; Golikand, A.N.; Mirershadi, S. Effect of Laser Wavelength at IR (1064 Nm) and UV (193 Nm) on the Structural Formation of Palladium Nanoparticles in Deionized Water. *The Journal of Physical Chemistry C* **2011**, *115*, 5049–5057, doi:10.1021/jp1091224.
24. Lopez, T.; Villa, M.; Gomez, R. UV-Visible Diffuse Reflectance Spectroscopic Study of Platinum, Palladium, and Ruthenium Catalysts Supported on Silica. *The Journal of Physical Chemistry* **1991**, *95*, 1690–1693, doi:10.1021/j100157a038.
25. Phillips, J.P.; Mackey, N.M.; Confait, B.S.; Heaps, D.T.; Deng, X.; Todd, M.L.; Stevenson, S.; Zhou, H.; Hoyle, C.E. Dispersion of Gold Nanoparticles in UV-Cured, Thiol–Ene Films by Precomplexation of Gold–Thiol. *Chemistry of Materials* **2008**, *20*, 5240–5245, doi:10.1021/cm8007842.
26. Zhao, X.; Zhan, X.; Zhang, H.; Wan, Y.; Yang, H.; Wang, Y.; Chen, Y.; Xie, W. Synthesis and Biological Evaluation of Isatin Derivatives Containing 1,3,4-Thiadiazole as Potent  $\alpha$ -Glucosidase Inhibitors. *Bioorganic & Medicinal Chemistry Letters* **2021**, *54*, 128447, doi:10.1016/j.bmcl.2021.128447
27. R. A. M. Al-Hasani MANNICH BASE DERIVED FROM 1,3,4-THIADIAZOLE AS CHELATING LIGAND FOR SOME TRANSITION METAL COMPLEXES. *ANJS* **2008**, *11*, 42–56, DOI:10.22401/JNUS.11.2.06.